Available online at www.sciencedirect.com
SCIENCE DIRECT
Sensors and Actuators A 128 (2006) 376–386
SENSORS AND ACTUATORS A PHYSICAL
www.elsevier.com/locate/sna

SiC cantilever resonators with electrothermal actuation

Liudi Jiang [a,*], R. Cheung [a], J. Hedley [b], M. Hassan [c], A.J. Harris [c], J.S. Burdess [b], M. Mehregany [d], C.A. Zorman [d]

[a] *School of Engineering and Electronics, Scottish Microelectronics Centre, The University of Edinburgh, King's Buildings, West Mains Road, Edinburgh EH9 3JF, UK*
[b] *School of Mechanical and Systems Engineering, University of Newcastle Upon Tyne, Newcastle NE1 7RU, UK*
[c] *School of Electrical, Electronics and Computer Engineering, University of Newcastle Upon Tyne, Newcastle NE1 7RU, UK*
[d] *Department of Electrical Engineering and Computer Science, Case Western Reserve University, Cleveland, OH 44106, USA*

Received 4 October 2005; received in revised form 23 January 2006; accepted 31 January 2006
Available online 10 March 2006

Abstract

Cubic SiC cantilever resonators designed for electrothermal actuation are presented. Metal electrodes with both open circuit and short circuit designs have been deposited and patterned on top of the 3C–SiC cantilevers. Pt electrodes on single crystal 3C–SiC cantilevers and NiCr electrodes on poly-crystalline 3C–SiC cantilevers have both been fabricated and tested in order to investigate the material property effect on the performance of the devices. An analytical model has been developed to understand the electrical power distribution in the cantilevers for the different material systems as well as the different metal terminations. Electrothermal actuation of resonance has been successfully achieved in all the fabricated cantilevers. The dynamic performance of the cantilever resonators has been systematically studied including resonance frequencies, amplitude response with voltage and actuation efficiencies. During the discussion of these results, the mechanism of the electrothermal actuation in these devices has been identified which allows actuation frequencies up to 100 MHz to be possible.

Keywords: Electrothermal actuation; SiC; Cantilever; Resonators

1. Introduction

Many methods for actuation of microelectromechanical system (MEMS) structures have been demonstrated, these include electrostatic, thermal, piezoelectric and electromagnetic. Among these methods, capacitive actuation has most commonly been used because of its low power consumption and short actuation times. However, capacitive actuation requires two electrodes separated by an insulator. One electrode is fixed and the other is attached or formed from the structure to be actuated. This requires the formation of a layered structure which in some cases can unnecessarily complicate the design and fabrication process and demands that the insulator be completely free of electrical shorts. A far simpler alternative is electrothermal actuation which only requires an electrical conductor to be deposited onto the surface of the structure to be actuated and the electrical power to be used to heat and hence mechanically strain the structure. Furthermore, capacitive actuation is often associated with a large closing gap in order to achieve high isolation and avoid pull-in [1,2] and stiction problems, which results in large actuation voltages [3]. In contrast, electrothermal actuation can be operated at relatively low voltages and is therefore compatible with standard IC voltage levels and it can also result in larger displacements and higher contact force with more compact structures [4]. These advantages of electrothermal actuation are particularly attractive for the actuation of MEMS switches [5], micromirrors [6], microtweezers [7] and AFM tips [8]. In addition, like capacitive actuation, electrothermal actuation can also function as a frequency mixer/filter due to the induced mechanical force being a function of the applied voltage squared [9].

Silicon Carbide (SiC) is a good candidate for microsensor and microactuator applications in harsh environments including locations of high temperature and abrasive and corrosive media. The progress on 3C–SiC deposition onto various large area substrates [10] and the development of surface micromachining

* Corresponding author. Tel.: +44 023 8059 8748; fax: +44 023 8059 3016.
E-mail address: ldjiang@soton.ac.uk (L. Jiang).

0924-4247/$ – see front matter © 2006 Elsevier B.V. All rights reserved.
doi:10.1016/j.sna.2006.01.045

Table 1
Dimensions and electrical properties of the cantilevers and electrodes

	Length (μm)	Width (μm)	Thickness (μm)	Resistivity (Ω cm)
Single crystal SiC cantilever	200	15	3	1.5
Pt electrodes	200	5	0.5	0.0017
Polycrystalline SiC cantilever	50	34	2	200
NiCr electrodes	50	7	0.28	0.0001

techniques for the fabrication of SiC devices [11,12] in recent years has stimulated the use of SiC as a structural material for MEMS. Due to its high Young's modulus and the relatively low mass density, SiC resonant structures can present much higher resonant frequencies compared to the same dimensioned Si or GaAs structures [13]. In addition, with a higher thermal conductivity than other conventional semiconductor materials, SiC MEMS can be heated and cooled more rapidly. These desirable properties of SiC suggest that electrothermally driven SiC resonant actuators can be particularly advantageous in many applications such as RF switches, AFM tips and mixer/filters where both high frequency and high mechanical performance are required. A variety of micromachined SiC resonators and microactuators have been developed and the majority of them reported to date employ electrostatic actuation [12,14]. To the best of our knowledge, there is little reported work on SiC electrothermally driven resonators.

In this paper, SiC cantilever resonators with electrothermal actuation have been designed and successfully fabricated using both single crystalline and polycrystalline 3C–SiC epitaxial films. These crystalline forms, which are grown on different substrates, differ in their mechanical properties and in their electrical properties (see Table 1), consequently, differences in device performance can be anticipated. Metal elements for carrying current have been deposited and patterned directly onto the SiC beam surface. The effect of the electrical termination (i.e. open circuit or short circuit) on the performance of the actuators has also been investigated.

2. Design considerations

Two basic electrothermal actuation designs are considered. These consist of suspended SiC cantilevers on top of which are metal elements with different terminations, as shown in the insets of Fig. 1.

2.1. Open circuit termination

In this case, the metal electrodes run along the top surface of the cantilever but are not connected at the free end, as shown in the inset of Fig. 1(a). In this design, the 3C–SiC layer is connected in series with the metal electrodes and therefore the power dissipated in both the metal electrodes and the SiC layer should contribute to the electrical heating of the cantilever.

2.2. Short circuit termination

In this form of termination, as shown in the inset of Fig. 1(b), the two electrodes are connected together at the free end of the cantilever. This design attempts to minimise the current through the 3C–SiC layer and hence its contribution to electrical heating.

3. Fabrication process

3.1. Pt/SiC cantilevers

These cantilevers were fabricated from nominally undoped 3 μm thick single crystal 3C–SiC film that was heteroepitaxially grown on a Si (1 0 0) wafer [15]. The details of their fabrication have been previously reported [11]. The cantilevers are 15 μm wide and 200 μm long. Focused ion beam (FIB) techniques were used to deposit platinum (Pt) with a thickness of 0.5 μm and a width of 5 μm on top of the beam to form the electrodes as the scanning electron microscope (SEM) micrographs for each form of termination shown in Fig. 1.

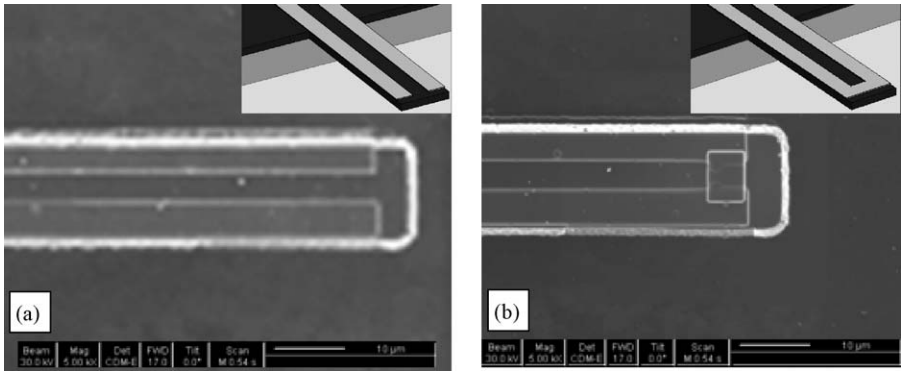

Fig. 1. SEM micrographs of fabricated SiC cantilever with platinum electrodes of (a) open circuit termination and (b) short circuit termination. The insets show the corresponding designs with different terminations of the top metal electrodes.

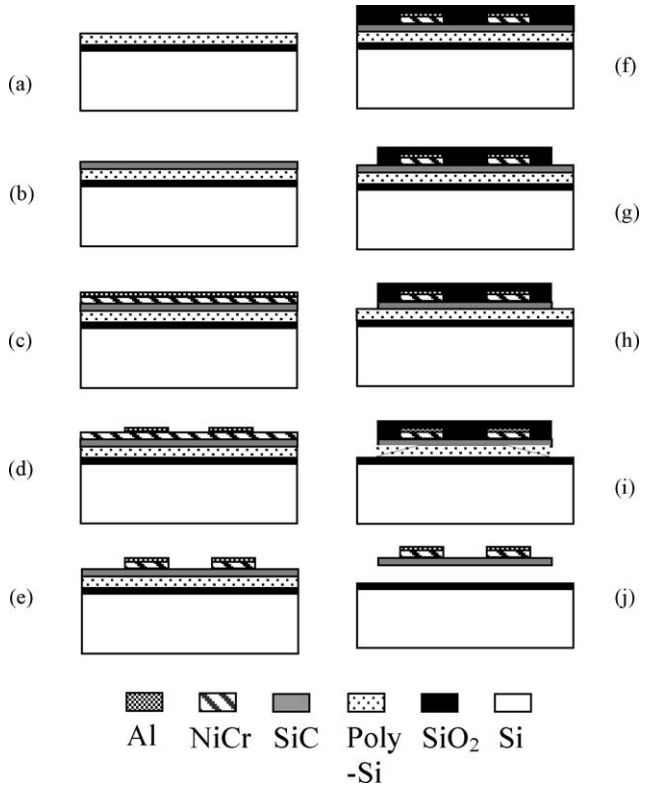

Fig. 2. Schematic process flow for the fabrication of NiCr/polySiC electrothermal cantilevers.

3.2. NiCr/polySiC cantilevers

In order to study the effect of the chosen metal and SiC materials on the performance of the devices, SiC cantilevers have also been fabricated from polycrystalline 3C–SiC which has been heteroepitaxially grown onto a substrate consisting of a 2 μm thick polycrystalline Si film deposited onto a thermally oxidized Si wafer of 100 mm diameter [16]. Fig. 2 shows the cross-sectional schematic illustration of the fabrication sequence. A 280 nm thick nichrome (NiCr) (Ni:Cr = 80%:20%) layer followed by a very thin Al layer was deposited onto the SiC. The purpose of the thin Al layer on top is to enable a good electrical contact during the later wire bonding process for the final devices. Photolithography has been performed to pattern the metal layers into the required electrode shapes. A 3 μm thick PECVD SiO_2 layer was used as a SiC etching mask. Suspended SiC cantilevers were obtained by etching in inductively coupled plasma using an SF_6/O_2 gas mixture. The plasma first anisotropically etched the SiC layer and then continued to isotropically etch the underlying poly-Si sacrificial layer until the cantilever was released [11]. The SiO_2 etch mask was then removed by reactive ion etching to expose the metal layer underneath. Electrical measurements have shown that the influence of the thin Al layer to the device properties was negligible. Fig. 3 shows typical SEM micrographs of the fabricated SiC cantilevers with both top views and side views. Reasonably straight cantilevers of 34 μm wide and of 50 μm long for both designs have been achieved.

4. Theoretical modelling

Electrothermal actuation of a cantilever results from mechanical strain induced by thermal expansion resulting from temperature variations due to electrical heating of an electrode attached to the surface of the cantilever. For a cantilever with thin electrodes, the mechanical strain either arises from the difference in thermal expansion coefficients between the electrode material and the cantilever material [17] or from a temperature gradient within the thickness of the cantilever [18], or a combination of both. In the case of the electrothermally actuated SiC cantilevers discussed in this paper, the materials used and their associated thermal expansion coefficients are approximately: SiC (2.5 E-6 K^{-1}), Pt (9 E-6 K^{-1}) and NiCr (14 E-6 K^{-1}) which are sufficiently different to permit both actuation mechanisms to exist. Since both single and polycrystalline SiC were grown in the same manner only with different substrates, no significant difference of the thermal expansion coefficients is expected to exist between them. The value quoted here is a representative value and will be used for both SiC crystalline forms.

4.1. Dynamic analysis

The electrical power dissipated in a resistance R is given by V^2/R. In general terms, if the device is actuated simultaneously

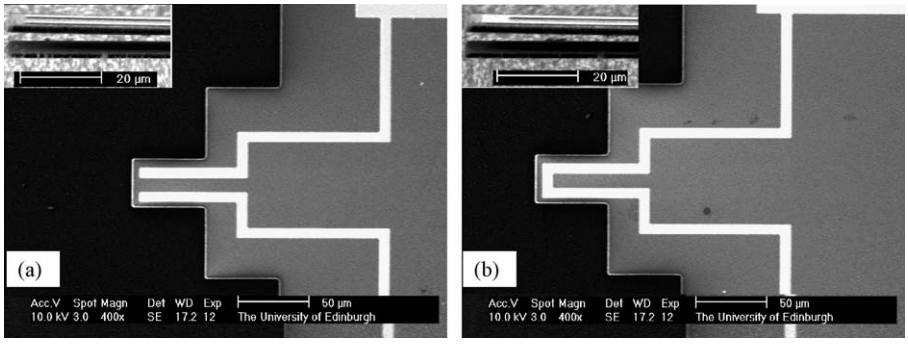

Fig. 3. SEM micrographs of the fabricated NiCr/polySiC of (a) open termination design and (b) short termination design. The insets show the side views of the cantilever end terminations.

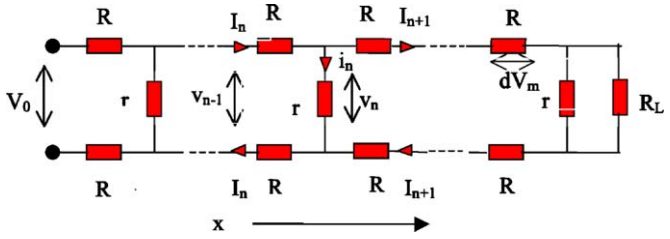

Fig. 4. Lumped resistance model for power distribution calculations.

by both an ac (V_{ac}) and a dc (V_{dc}) voltage, then V^2 is given by

$$V^2 = (V_{ac}\sin\omega_{ac}t + V_{dc})^2 = 2V_{ac}V_{dc}\sin\omega_{ac}t + 0.5V_{ac}^2(1-\cos 2\omega_{ac}t) + V_{dc}^2 \quad (1)$$

where ω_{ac} is the angular frequency of the applied V_{ac}. Under these conditions, resonance will be achieved via the $V_{ac}V_{dc}$ term in (1) when the electrothermal actuation frequency is the same as the mechanical resonance frequency (f_0). If only V_{ac} is applied, actuation will occur via the V_{ac}^2 term which will require that $f_{ac} = 0.5f_0$. With both forms of actuation, the vibration amplitude of a mode should be linearly dependent on the corresponding actuation term in (1).

4.2. Power distribution

Both Pt patterned single crystalline SiC and NiCr patterned polycrystalline SiC cantilever resonators have been formed and studied in this work. The dimensions and electrical properties of the materials are listed in Table 1. The resistivities quoted are typical values for these materials produced in our laboratories for this work.

In order to determine the power distribution along a cantilever and also the division of power between the metal and the SiC layers, the electrical circuit of the SiC cantilever and its electrodes was represented by the lumped resistance model shown in Fig. 4. Here, R and r are the resistances of the metal electrode and SiC, respectively, over a distance dx along the cantilever length and R_L is the termination resistance at the end of the cantilever.

In this model the dimensions and resistivities of the metal and SiC layers are represented as follows: H is the length of SiC between metal electrodes, d_2 the thickness of SiC cantilever, h the width of metal electrode, d_1 the thickness of metal electrode, L the length of cantilever, ρ_1 the resistivity of metal, and ρ_2 is the resistivity of SiC.

From the circuit in Fig. 4 we can deduce that,

$$V_n = r(I_n - I_{n+1}) \quad \text{and} \quad I_n = \frac{V_{n-1}-V_n}{2R}; \quad I_{n+1} = \frac{V_n - V_{n+1}}{2R} \quad (2)$$

therefore,

$$V_{n+1} - 2\left(1+\frac{R}{r}\right)V_n + V_{n-1} = 0 \quad (3)$$

The solution to the above equation is of the form $V_n = \alpha k^n$ from which k can be found as

$$k = \left(1+\frac{R}{r}\right) \pm \sqrt{\left(1+\frac{R}{r}\right)^2 - 1} \quad (4)$$

Since

$$\frac{R}{r} = \frac{\rho_1 d_2}{d_1 h \rho_2 H}\,\mathrm{d}x^2 = \lambda^2\,\mathrm{d}x^2 \quad (5)$$

where

$$\lambda = \left[\frac{\rho_1 d_2}{d_1 h \rho_2 H}\right]^{1/2} \quad (6)$$

The two solutions for k can be written to the order dx^2 as

$$k_1 = 1 - \sqrt{2}\lambda\,\mathrm{d}x + \lambda^2\,\mathrm{d}x^2; \quad k_2 = 1 + \sqrt{2}\lambda\,\mathrm{d}x + \lambda^2\,\mathrm{d}x^2 \quad (7)$$

If the solution for V_n is expressed as

$$V_n = \alpha_1 k_1^n + \alpha_2 k_2^n \quad (8)$$

it may be shown that Eq. (3) can be rewritten as

$$\frac{\mathrm{d}^2 V}{\mathrm{d}^2 x} = 2\lambda^2 V \quad (9)$$

the solution of which is given by

$$V(x) = \mathrm{A}\mathrm{e}^{-\sqrt{2}\lambda x} + \mathrm{B}\mathrm{e}^{+\sqrt{2}\lambda x} \quad (10)$$

Applying the boundary conditions to determine the constants A and B, when $x = 0$, namely at the root of the cantilever,

$$V(0) = V_0 = A + B \quad (11)$$

When $x = L$, namely at the free end of the cantilever,

$$V(L) = I(R_L||r) = \frac{\mathrm{d}V_m}{R}(R_L||r) = \frac{\mathrm{d}V_{x=L}}{2R}(R_L||r) = \mu\left.\frac{\mathrm{d}V}{\mathrm{d}x}\right|_{x=L} \quad (12)$$

where

$$\mu = \frac{h_1 d_1}{2\rho_1}R_L \quad (13)$$

Therefore in general,

$$V(x) = V_0\frac{(1+\sqrt{2}\lambda\mu)}{\Delta}\mathrm{e}^{+\sqrt{2}\lambda(L-x)} - V_0\frac{(1-\sqrt{2}\lambda\mu)}{\Delta}\mathrm{e}^{-\sqrt{2}\lambda(L-x)} \quad (14)$$

where

$$\Delta = 2\sinh\sqrt{2}\lambda L + 2\sqrt{2}\lambda\mu\cosh\sqrt{2}\lambda L \quad (15)$$

We can therefore conclude that power dissipation in SiC layer per unit length at x is

$$P_{SiC}(x) = \frac{V(x)^2}{r\,\mathrm{d}x} = \frac{d_2}{\rho_2 H}V(x)^2 \quad (16)$$

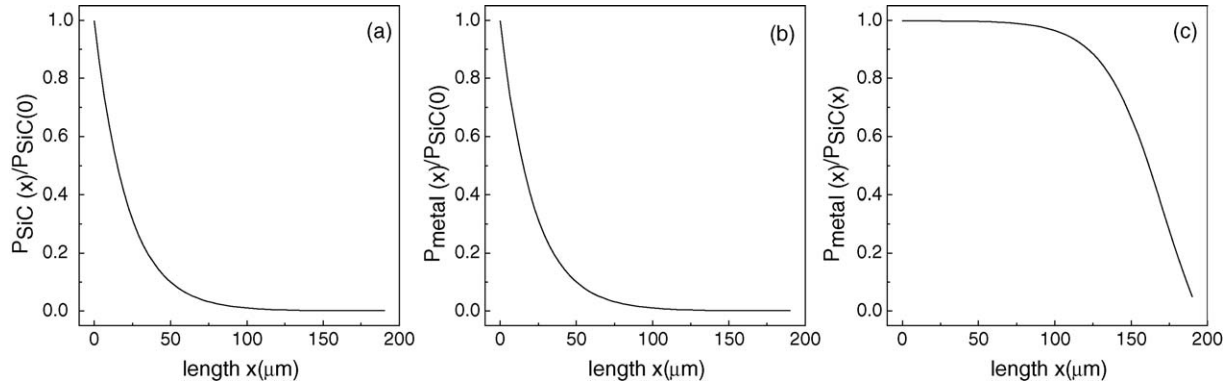

Fig. 5. Power dissipation along the length of the Pt/SiC cantilever with open circuit termination (a) in SiC (b) and in Pt (c) ratio between Pt and SiC.

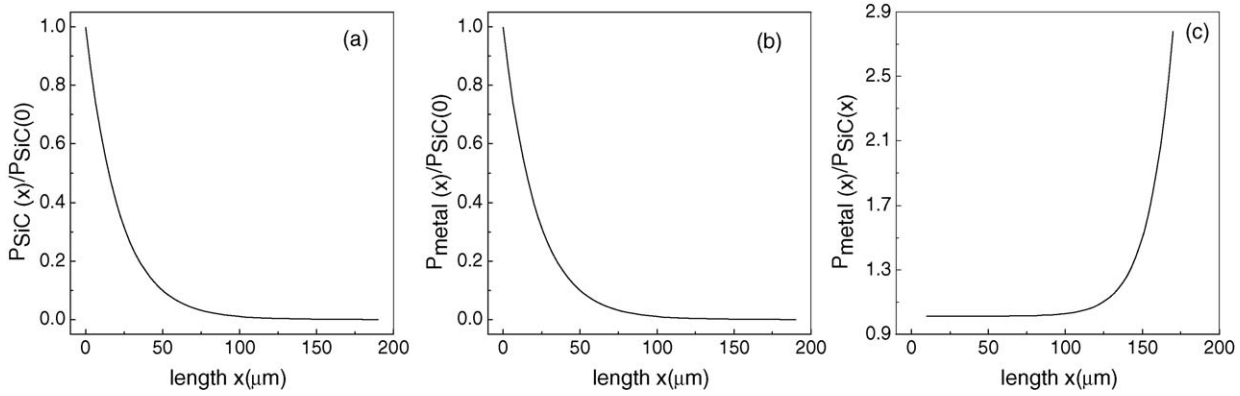

Fig. 6. Power dissipation along the length of the Pt/SiC cantilever with short circuit termination (a) in SiC (b) in Pt and (c) ratio between Pt and SiC.

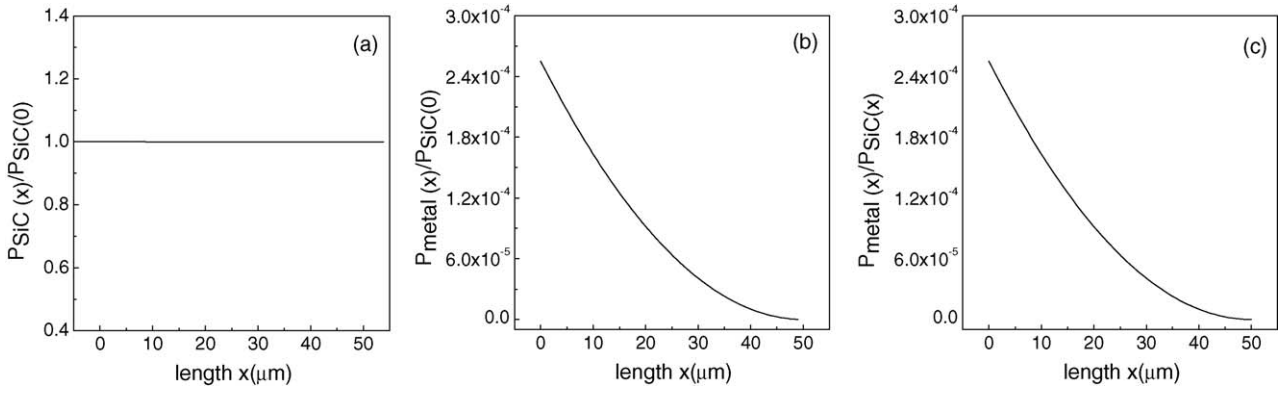

Fig. 7. Power dissipation along the length of the NiCr/polySiC cantilever for open circuit termination (a) in SiC (b) in NiCr and (c) ratio between NiCr and SiC.

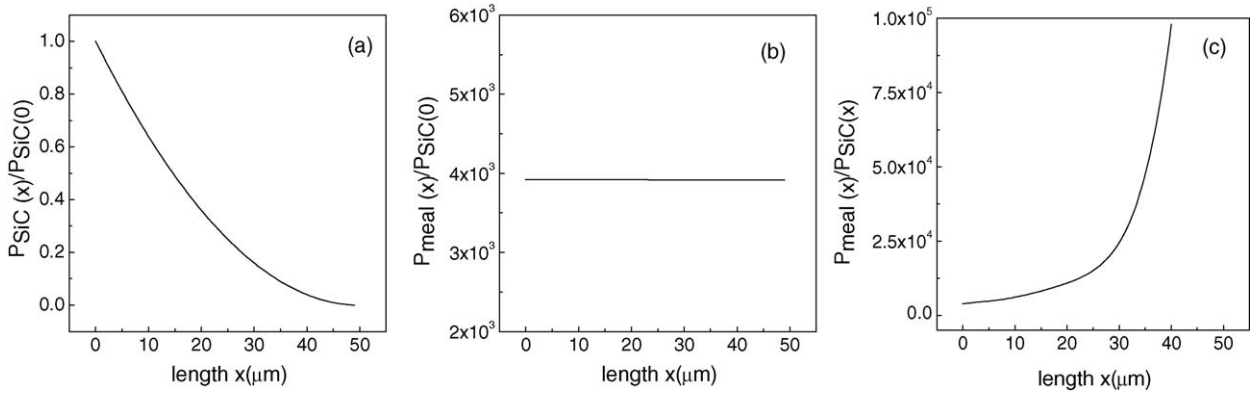

Fig. 8. Power dissipation along the length of the NiCr/polySiC cantilever for short circuit termination (a) in SiC (b) in NiCr (c) and ratio between NiCr and SiC.

Table 2
Ratios of resistivities and corresponding values of X_0 for metal/SiC cantilevers

Device materials	ρ_2/ρ_1	X_0 (μm)
Pt/single crystal SiC	882	43
NiCr/polycrystalline SiC	2E6	3130

Power dissipated in metal layer per unit length at x is

$$P_{\text{metal}}(x) = \frac{\mathrm{d}V(x)^2}{2R\mathrm{d}x} = \frac{d_1 h}{2\rho_1}\left(\frac{\mathrm{d}V(x)}{\mathrm{d}x}\right)^2 \tag{17}$$

4.2.1. Open circuit termination

In this case, $R_L = \infty$ and $\mu \gg 1$ giving $\Delta = 2\sqrt{2}\lambda\mu \cosh \sqrt{2}\lambda L$ and from (16):

$$\frac{P_{\text{SiC}}(x)}{P_{\text{SiC}}(0)} = \frac{\cosh^2(L-x)/X_0}{\cosh^2(L/X_0)} \tag{18}$$

where the critical length

$$X_0 = \frac{1}{\sqrt{2}\lambda} \tag{19}$$

and

$$P_{\text{SiC}}(0) = \frac{V_0^2}{\rho_2 H/d_2} \tag{20}$$

and from (17),

$$\frac{P_{\text{metal}}(x)}{P_{\text{SiC}}(0)} = \frac{\sinh^2(L-x)/X_0}{\cosh^2(L/X_0)} \tag{21}$$

From (18) and (21) the ratio of $P_{\text{metal}}(x)/P_{\text{SiC}}(x)$ is given by

$$\frac{P_{\text{metal}}(x)}{P_{\text{SiC}}(x)} = \tanh^2\frac{(L-x)}{X_0} \tag{22}$$

4.2.2. Short circuit termination

In this case, $R_L = 0$ and $\mu = 0$ which gives $\Delta = 2\sinh\sqrt{2}\lambda L$ and from (16)

$$\frac{P_{\text{SiC}}(x)}{P_{\text{SiC}}(0)} = \frac{\sinh^2(L-x)/X_0}{\sinh^2(L/X_0)} \tag{23}$$

and from (17)

$$\frac{P_{\text{metal}}(x)}{P_{\text{SiC}}(0)} = \frac{\cosh^2(L-x)/X_0}{\sinh^2(L/X_0)} \tag{24}$$

From (23) and (24) the ratio of $P_{\text{metal}}(x)/P_{\text{SiC}}(x)$ given by

$$\frac{P_{\text{metal}}(x)}{P_{\text{SiC}}(x)} = \frac{1}{\tanh^2(L-x)/X_0} \tag{25}$$

From Eqs. (6) and (19) and values provided in Table 1, the critical length X_0 in both Pt/SiC and NiCr/polySiC cantilevers have been calculated and are listed in Table 2. It is obvious that the significant difference in the X_0 values of the two material systems results from the large difference in the ratio of the resistivities. Using Eqs. (18)–(25), the power dissipated in the SiC and the metal electrodes have been calculated and are presented in Figs. 5–8.

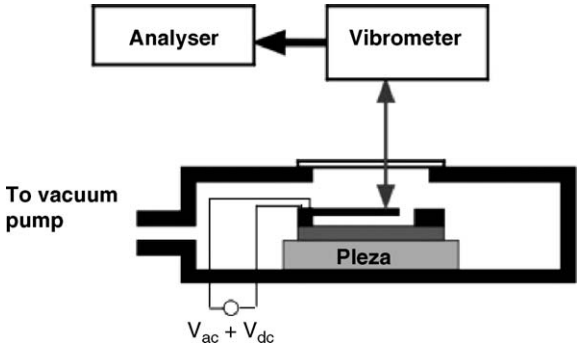

Fig. 9. Dynamic measurement system.

In the Pt/SiC system, the power dissipated in the SiC and Pt decreases rapidly along the beam due to the relatively short critical length X_0, compared to the length of the cantilever. The power distribution along the cantilever is unaffected by the terminations due to the power not reaching the end of the cantilever. Over the initial part of the cantilever, the power dissipated per unit length in the Pt and the SiC are almost equal.

In the NiCr/polySiC cantilever, there is a profound difference between the short circuit and open circuit terminations due to the relatively large value of X_0, compared to the length of cantilever, making the distribution of power sensitive to the termination. In the open circuit case, the power is mainly dissipated in the SiC and is uniform along the cantilever. In the short circuit case, the power is once again uniformly distributed along the cantilever but in this case almost entirely in the NiCr.

The substantial difference between the two material systems is clearly due to the considerable difference in X_0 which results from the relative values of the resistivities of the 3C–SiC and metal used.

5. Test results and discussion

5.1. Metal/SiC contact

For those situations where the current passes through the SiC, the electrical characteristics of the contact at the metal/SiC interface are important. In particular, for a given supply voltage, high contact resistance can unnecessarily limit the current through the device, and hence limit its actuation performance. Furthermore, if the contact is rectifying then this will modify the frequency content of the drive signal again making the thermal actuation of a mechanical resonance inefficient. Ohmic contacts were verified for both material systems by conducting *I–V* measurements on the open circuit terminated devices which showed linear responses passing through the origin.

5.2. Dynamic performance

The electrothermal actuation of the fabricated SiC cantilever resonators was tested at room temperature using the arrangement shown in Fig. 9. The measurement chamber pressure was kept at less than 1 mBar in order to eliminate damping of the resonance due to the air. A combination of a sinusoidal V_{ac} and a V_{dc}

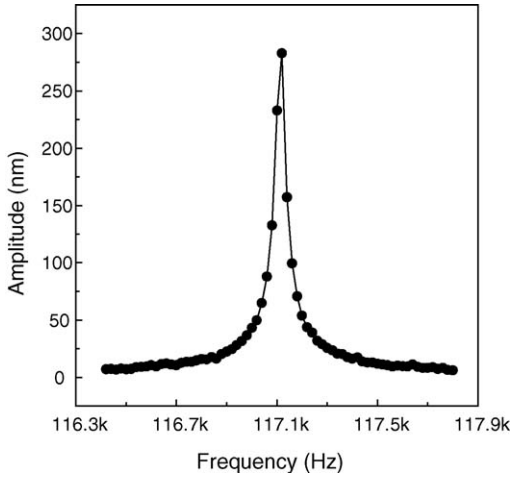

Fig. 10. Fundamental resonance peak of the Pt/SiC cantilever by electrothermal actuation with $V_{dc} = 0.2$ V and $V_{ac} = 0.3$ V_{pp} (V_{pp} represents peak to peak voltage).

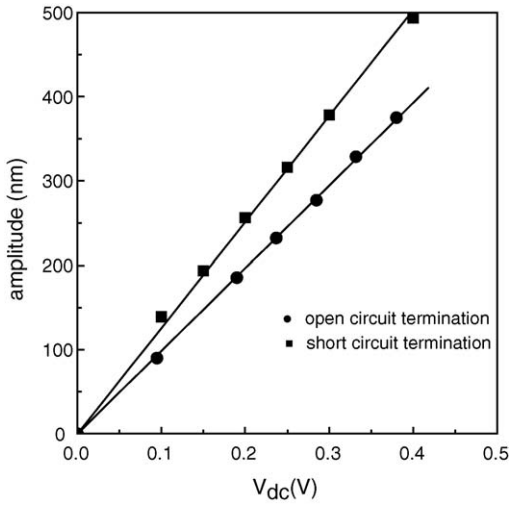

Fig. 12. The amplitude of the fundamental resonance peak for the Pt/SiC cantilevers as a function of V_{dc} when $V_{ac} = 0.1$ V_{pp}.

was applied to the metal electrodes using an HP 33120A function/arbitrary waveform generator. The dynamic vibration of the beams as a function of applied V_{ac} frequency f_{ac} was optically detected using a Polytec OFC 3000 vibrometer. The velocity of the deflection was measured in the first instance which was then translated into displacement with sub-nanometer resolution. The detail of the measurement setup has also been described elsewhere [19,20].

5.2.1. Resonance frequencies

Resonance of the fundamental mode was observed by electrothermal actuation when the applied f_{ac} was nominally 117.12 and 897.40 kHz for the Pt/SiC and NiCr/polySiC cantilevers, respectively. The resonance peaks are shown in Figs. 10 and 11. A small shift in resonance frequency was induced by the change in the electrode terminations due to the increase in effective mass of the cantilever. Actuation of the fundamental resonance was also confirmed by applying V_{ac} at a frequency equal to half the fundamental resonance frequencies of the cantilevers. These results confirm the V^2 actuation response expected from Eq. (1).

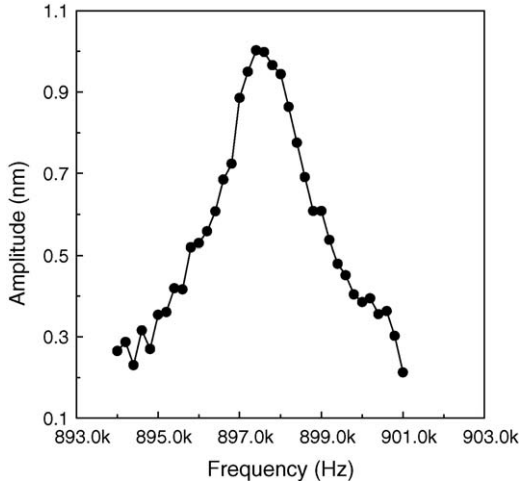

Fig. 11. Fundamental resonance peak by electrothermal actuation of the NiCr/polySiC cantilever with open circuit termination ($V_{dc} = 1$ V and $V_{ac} = 2$ V_{pp}).

5.2.2. Voltage response

The vibration amplitude of the cantilevers for both material systems and terminations was investigated as a function of the applied voltages V_{ac} and V_{dc}, respectively. A linear dependence of the amplitude on the applied voltages was observed when f_{ac} equals the fundamental resonance frequencies of the cantilevers. This linear behaviour as a function of V_{dc} is shown in Figs. 12 and 13. These results are in keeping with Eq. (1) and a linear electrothermal actuation response.

5.2.3. Actuation efficiency

When a mixed voltage ($V_{ac} + V_{dc}$) was applied to the devices at the resonance frequency of the cantilevers, the peak actuation power $2V_{ac}V_{dc}$ resulted in electrical heating and this caused dynamic vibration of the cantilevers. Using the data presented in Figs. 12 and 13, the electrothermal actuation efficiency of the fundamental resonance has been calculated by dividing the vibration amplitude at the free end of the cantilevers by the peak actuation power, i.e. $2V_{ac}V_{dc}/R_{total}$, where R_{total} is the resistance of the devices measured between the two metal pads of each cantilever. The results from both material systems and terminations are given in Table 3.

In the case of Pt/SiC cantilevers, the actuation efficiency remains almost independent of the electrical termination. This is in agreement with the calculated power distribution along the length of the cantilever being independent of the termination due to the critical length X_0 being only a small fraction (22%) of the length of the cantilever.

In the case of NiCr/polySiC cantilevers, the actuation efficiency is significantly greater for the short circuit case. The power distribution model, described in Section 4, has revealed that the power is mainly dissipated in the NiCr for the short circuit case whilst the power is mainly dissipated in the SiC for the open circuit case. This is due to X_0 being many times (63

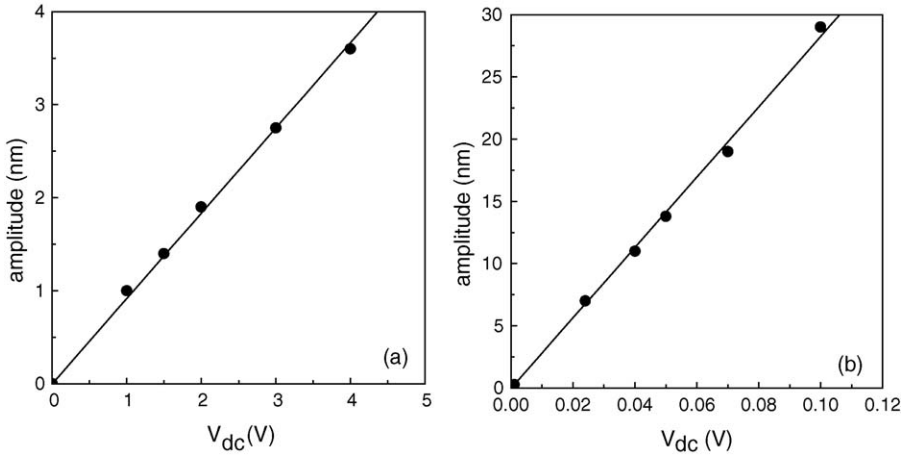

Fig. 13. The amplitude of the fundamental resonance peaks as a function of V_{dc} for the NiCr/polySiC cantilevers with (a) open circuit termination ($V_{ac} = 2.0\ V_{pp}$) and (b) short circuit termination ($V_{ac} = 0.048\ V_{pp}$).

times) the length of the cantilever. The much greater actuation efficiency in the short circuit case therefore indicates that the heat generated in the NiCr is a more efficient source of heat for electrothermal actuation than that generated in the SiC. In the latter case, bulk heating of the SiC is present and only a small temperature gradient is expected in the SiC and NiCr layers. Under these approximately uniform heating conditions, actuation due to a difference in thermal expansion coefficients would be expected to dominate. Since the actuation efficiency is at its lowest for this situation (open circuit termination), one can conclude that the greater actuation efficiency observed when the power is dissipated in the metal (short circuit termination) arises from a temperature gradient through the thickness of the SiC cantilever induced by heating of the metal at its surface. The effect of a temperature gradient will therefore add to any actuation arising from a difference in thermal expansion coefficients. This conclusion is also expected to be applicable to the Pt/SiC devices. For actuation via a temperature gradient, the turn over frequency (f_t) at which the actuation efficiency starts to decrease with increase frequency is given by $1.9k/\rho cd^2$, were k is the thermal conductivity of the cantilever material, ρ is its density, d is the thickness and c is its specific heat [18]. The calculated f_t is 35 and 78 MHz for the Pt/SiC ($d = 3\ \mu m$) and NiCr/polySiC ($d = 2\ \mu m$), respectively using $k = 360\ W\ m^{-1}\ K^{-1}$, $\rho = 3170\ kg\ m^{-3}$, $c = 690 J\ kg^{-1}\ K^{-1}$. Since the fundamental frequencies of the two cantilevers (Pt/SiC and NiCr/PolySiC) studied here are significantly below these values, the difference in their actuation efficiencies cannot be explained in terms of a reduction in the heat induced mechanical force with frequency. The remaining factors which can contribute to the difference in the actuation efficiencies include the magnitude of the induced temperature gradient and the distribution of heating along the cantilever length which controls the distribution of thermally induced mechanical forces that drive the cantilevers into resonance. The distribution of heating in the Pt/SiC cantilever is concentrated near its root which is known to be a more efficient location for inducing strain to excite the fundamental mode and therefore will in part account for the higher actuation efficiency in the Pt/SiC cantilever.

Table 3
Actuation efficiencies for both material systems and terminations

Material/design	R (Ω)	Actuation efficiency (nm/μW)
Pt/SiC cantilever with open circuit termination	1.2 k	6
Pt/SiC cantilever with short circuit termination	1.1 k	7
NiCr/polySiC cantilever with open circuit termination	18.2 k	4×10^{-3}
NiCr/polySiC cantilever with short circuit termination	41	90×10^{-3}

5.2.4. *Variation of resonance frequency with actuation voltage*

It was observed that the fundamental resonant frequencies of electrothermally actuated NiCr/polySiC cantilevers decreased slightly with the applied actuation voltage. Fig. 14 shows that the frequency decreases by 12 ppm when the applied V_{dc} is

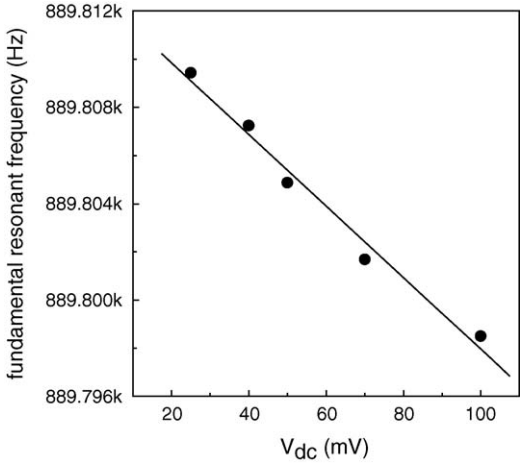

Fig. 14. The shift of the fundamental resonance frequency vs. input V_{dc} ($V_{ac} = 48\ mV_{pp}$) for a NiCr/polySiC cantilever with short circuit termination.

increased from 25 to 100 mV. In contrast to a bridge type structure, thermal tensile stresses are not induced in a cantilever and therefore it should have no effect on the resonant frequencies of the cantilevers. A similar decrease has been observed in other NiCr/poly3C–SiC cantilevers by increasing the temperature of the cantilever and consequently, we believe the decrease in resonant frequency with voltage is mainly due to the decrease in the elastic moduli of the 3C–SiC and NiCr with increase in temperature against a background of a small increase in frequency due to dimensional changes [21,22]. A decrease in frequency of 12 ppm was therefore found to correlate with an average increase of 0.3 °C in temperature.

6. Conclusion

3C–SiC cantilever resonators were successfully fabricated from single crystalline and polycrystalline 3C–SiC films and electrothermally actuated into resonance. The electrothermal response of the devices showed a linear dependence of the resonance amplitude on peak actuating power.

The effect of the termination of the metal electrodes on the power distribution along the cantilever is governed by the relative values of the resistivities of the metal and SiC used which determines the critical length X_0 for thermal actuation. In the NiCr/polySiC device, the ratio of the two resistivities (SiC/metal) was ~2268 times greater than the ratio for the Pt/SiC device. This was mainly due to the substantial difference in the resisitivities of the two forms of SiC being amplified by the more modest difference in the metal resistivities. This resulted in the heat being confined to the root of the Pt/SiC cantilevers, whilst, for the NiCr/polySiC cantilevers, the power dissipation was spread uniformly along the whole cantilever length. This was in part responsible for the greater actuation efficiency observed in the Pt/SiC devices due to the induced strain being at the root of the cantilever where the modes of vibration are more effectively excited.

From interpreting the actuation efficiency measurements of the devices with the power distribution model it was deduced that a temperature gradient through the thickness of the SiC cantilever which was induced by heating of the metal was the main mechanism responsible for electrothermal actuation. With this actuation mechanism, SiC cantilevers with thicknesses in the micron region can be expected to be actuated at frequencies up to a 100 MHz without any loss in actuation efficiency [18].

The resonance frequency of the fundamental mode slightly decreased with increase in applied voltage. This was explained as being mainly due to the elastic moduli of SiC and NiCr decreasing with increase in temperature. Besides being a useful indicator of average device temperature which in this case was less than one degree centigrade, this could also be potentially advantageous for the post-package fine tuning of the electrothermal SiC resonators.

Acknowledgement

This work was supported by Engineering and Physical Sciences Research Council (EPSRC) Grant No. GR/R38019/01.

References

[1] K.E. Petersen, Micromechanical membrane switches on silicon, IBM J. Res. Dev. 23 (1979) 376–385.
[2] W. Riethmuller, W. Benecke, Thermally excited silicon microactuators, IEEE Trans. Elec. Dev. 35 (1988) 758–763.
[3] Y. Wang, Z. Li, D.T. McCormick, N.C. Tien, A micromachined RF microrelay with electrothermal actuation, Sensor Actuator A 103 (2003) 231–236.
[4] L. Que, J.S. Park, Y.B. Gianchandani, Bent-beam electro-thermal actuators for high force applications, in: Proceedings of the Twelfth IEEE International Conference on Micro Electro Mechanical Systems, 1999, pp. 31–36.
[5] B. Ketterer, B. Bitnar, B. Haas, T. Neiger, D. Bachle, F. Glaus, J. Gobrecht, Electromechanical microswitches with thermal actuation, in: Proceedings of the International Microprocesses and Nanotechnology Conference, 2002, pp. 206–207.
[6] A. Jain, A. Kopa, Y. Pan, G.K. Fedder, H. Xie, A two-axis electrothermal micromirror for endoscopic optical coherence tomography, IEEE J. Sel. Top. Quant. Electron. 10 (2004) 636–642.
[7] E.V. Bordatchev, S.K. Nikumb, Microgripper: design, finite element analysis and laser microfabrication, in: Proceedings of International Conference on MEMS, Nano and Smart Systems, 2003, pp. 308–313.
[8] R. Pedrak, T. Ivanov, K. Ivanova, T. Gotszalk, N. Abedinov, I.W. Rangelow, K. Edinger, E. Tomerov, T. Schenkel, P. Hudek, Micromachined atomic force microscopy sensor with integrated piezoresistive sensor and thermal bimorph actuator for high-speed tapping-mode atomic force microscopy phase-imaging in higher eigenmodes, J. Vac. Sci. Technol. B 21 (2003) 3102–3107.
[9] M.A. Hassan, Silicon Carbide MEMS Characterisation and Actuation of 3C-SiC Cantilevers and Bridges, Ph.D. Thesis, University of Newcastle, England, 2005.
[10] C.A. Zorman, M. Mehregany, Silicon carbide for MEMS and NEMS – an overview, Proc. IEEE 2 (2002) 1109–1114.
[11] L. Jiang, R. Cheung, M. Hassan, A.J. Harris, J.S. Burdess, C.A. Zorman, M. Mehregany, Fabrication of SiC microelectromechanical systems using one-step dry etching, J. Vac. Sci. Technol. B 21 (2003) 2998–3001.
[12] L. Jiang, M. Hassan, R. Cheung, A.J. Harris, J.S. Burdess, C.A. Zorman, M. Mehregany, Dry release fabrication and testing of SiC electrostatic cantilever actuators, Microelectron. Eng. 78/79 (2005) 106–111.
[13] Y.T. Yang, K.L. Ekinci, X.M. Huang, L.M. Schiavone, M.L. Roukes, C.A. Zorman, M. Mehregany, Monocrystalline silicon carbide nanoelectromechanical systems, Appl. Phys. Lett. 78 (2001) 162–164.
[14] A.A. Yasseen, C.H. Wu, C.A. Zorman, M. Mehregany, Fabrication and testing of surface micromachined polycrystalline SiC micromotors, IEEE Electron Dev. Lett. 21 (2000) 164–166.
[15] C.A. Zorman, A.J. Fleischman, A.S. Dewa, M. Mehregany, C. Jacob, P. Pironz, Epitaxial growth of 3C–SiC films on 4 in. diam (1 0 0) silicon wafers by atmospheric pressure chemical vapor deposition, J. Appl. Phys. 78 (1995) 5136.
[16] C.A. Zorman, S. Roy, C.H. Wu, A.J. Fleischman, M. Mehregany, Characterization of polycrystalline silicon carbide films grown by atmospheric pressure chemical vapour deposition on polycrystalline silicon, J. Mater. Res. 13 (1998) 406–412.
[17] M.B. Othman, A. Brunnschweiler, Electrothermally excited silicon beam mechanical resonators, Electron. Lett. 23 (1987) 728–730.
[18] T.S.J. Lammerink, M. Elwenspoek, J.H.J. Fluitman, Frequency dependence of thermal excitation of micromechanical resonators, Sensor Actuator A 25–27 (1991) 685–689.
[19] J. Hedley, A.J. Harris, J.S. Burdess, M.E. McNie, The development of a "workstation" for optical testing and modification of IMEMS on a wafer, in: SPIE Proceedings on Design, Test and Packaging of MEMS/MOEMS, vol. 4408, 2001, pp. 402–408.
[20] J.S. Burdess, A.J. Harris, D. Wood, R.J. Pitcher, D. Glennie, A system for the dynamic characterization of microstructures, IEEE J. Microelectromech. Syst. 6 (1997) 322–328.

[21] A.J. Fleischman, S. Roy, C.A. Zorman, M. Mehregany, Behavior of polycrystalline SiC and Si surface-micromachined lateral resonant structures at elevated temperatures, Mater. Sci. Forum 264–268 (1998) 889–892.
[22] J. Han, C. Zhu, J. Liu, Y. He, Dependence of the resonance frequency of thermally excited microcantilever resonators on temperature, Sensor Actuator A 101 (2002) 37–41.

Biographies

Liudi Jiang received her PhD in advanced material analysis from the University of Dundee in 2001. Since then, Dr. Jiang has held the post of research fellow in the Scottish Microelectronics Center at the University of Edinburgh where she was a key contributor to research aiming towards the optimisation of SiC dry etch processes and the development of state-of-art SiC electronic devices and microelectromechanical systems (MEMS). During which time, she has also been a visiting researcher working for 6 weeks at Delft Institute of Microelectronics and Submicron Technology in Delft University of Technology. Dr. Jiang is currently a postdoctoral researcher at the University of Southampton. Her current research interests include the development of nanoelectromechanical systems (NEMS) from novel semiconductor materials and 3D integrations. She has so far published over 30 high standard papers in international journals and has one patent application pending.

R. Cheung obtained a first class honours degree and a PhD in Electronics and Electrical Engineering from the University of Glasgow. She has worked at IBM Thomas J. Watson Research Centre in Yorktown Heights, USA; Delft Institute of Microelectronics and Submicron Technology, The Netherlands; Laboratory for Electromagnetic Fields and Microwave Electronics, ETHZ, Switzerland and the University of Canterbury, New Zealand. Dr. Cheung worked on various topics related to semiconductor technology, nanoelectronics, mesoscopic physics and microwave circuits. Currently, she is a reader at the Institute of Integrated Micro and Nano Systems within the School of Engineering and Electronics at the University of Edinburgh. Her present research interests are in silicon carbide microelectromechanical systems and carbon nanotube electronics.

J. Hedley received a PhD in atomic physics from the University of Newcastle in 1996. He has subsequently been employed as a postdoctoral researcher in MEMS design, fabrication and testing. He is currently a lecturer at the University of Newcastle in the School of Mechanical and Systems Engineering. His research interests are in MEMS/NEMS metrology and biosensors.

M. Hassan received the BEng (honors) in mechatronics engineering from International Islamic University, Malaysia in 1999, and the MSc (distinction) in automation and control from Newcastle University, Newcastle Upon Tyne, UK, 2001. He recently submitted a PhD Dissertation entitled, "Silicon Carbide MEMS: characterization and actuation of 3C–SiC cantilevers and bridges" for graduation on May 2006.

A.J. Harris (PhD and BSc(Tech) University of Wales) is a lecturer in the School of Electrical, Electronic and Computer Engineering at the University of Newcastle, England. His research interests include microelectromechanics, optoelectronics, sensors and actuators. Current research includes the development of optical testing and processing methods and the application of vibratory structures to the production of physical and biological sensors. This work is in collaboration with other members of the Institute for Nanoscale Science and Technology.

J.S. Burdess is Professor of Engineering Dynamics in the School of Mechanical and System Engineering at the University of Newcastle. Over the last 30 years he has had a research interest in the dynamics of vibratory systems and the design and analysis of gyroscopic sensors and has acted as a consultant to industry on these subjects. The work on vibration has included the dynamics of non-linear and parametrically excited resonators, surface wave and other acoustic resonators, methods of vibration control and the dynamic behaviour of power transmission systems. The research into inertial devices has covered the analysis and design of navigational quality gyroscopes, such as the dynamically tuned gyroscope, and lower performance rate devices such as the vibrating piezoelectric cylinder gyro and a number of vibratory MEMS designs. Recently Professor Burdess has developed a research interest in MEMS and is an active member of the University's Institute of Nano-Science and Technology. This work was developed via projects on rate sensors and now includes projects on:

- Rapid deep etching process for SiC and the design & fabrication of sensors.
- Silicon bioMEMS sensors employing resonant structures and beam deflection methods.
- Methods of tuning vibratory MEMS structures via ablation and active methods.
- Optical measurement of MEMS structures and its extension to the nanometer scale and frequencies in excess of 20 MHz (static-profilometry with electrostatic deflection and dynamic – Doppler and stroboscopic profilometry).

Funding for this MEMS research is provided by EPSRC, BBSRC, DTI and QinetiQ and is supported by five members of academic staff and four postgraduate students.

M. Mehregany received his BS in Electrical Engineering from the University of Missouri in 1984, and his MS and PhD in Electrical Engineering from Massachusetts Institute of Technology in 1986 and 1990, respectively. From 1986 to 1990, he was a consultant to the Robotic Systems Research Department at AT&T Bell Laboratories, where he was a key contributor to ground-breaking research in microelectromechanical systems (MEMS). In 1990, he joined the Department of Electrical Engineering and Applied Physics at Case Western Reserve University as an Assistant Professor. He was awarded the Nord Assistant Professorship in 1991, was promoted to Associate Professor with tenure in July 1994, and was promoted to Full Professor in July 1997. He held the George S. Dively Professor of Engineering endowed chair from January 1998 until July 2000, when he was appointed the Goodrich Professor of Engineering Innovation. He served as the Director of the MEMS Research Center at Case from July 1995 until December 2002. Since January 2003, Professor Mehregany has been serving as Chairman of the Electrical Engineering and Computer Science Department. Professor Mehregany is well known for his research in the area of MEMS, and his work has been widely covered by domestic and foreign media. He has over 250 publications describing his work, holds 15 U.S. patents, and is the recepient of a number of awards/honors. He served as the Editor-in-Chief of the Journal of Micromechanics and Microengineering from January 1996 to December 1997, and is Assistant-to-the-President of the Transducers Research Foundation. His research interests are in micro- and nano-electromechanical systems (MEMS and NEMS), including sensors, actuators, micromachining and microfabrication technologies. His additional specialized interest centers on developing silicon carbide as an enabling material for MEMS and NEMS, in particular for applications in harsh environments. Professor Mehregany is the founder/cofounder of several technology companies, including Advanced Micromachines Incorporated (now part of The Goodrich Corporation), FLX Micro Inc. (http://www.flxmicro.com) and NineSigma Inc. (http://www.ninesigma.com).

C.A. Zorman, PhD received his BS cum laude in physics and BA cum laude in economics from the Ohio State University in 1988, and MS and PhD in physics from Case Western Reserve University in 1991 and 1994, respectively. His doctoral research involved an investigation of the secondary electron emission properties of CVD diamond films for vacuum electronics. Dr. Zorman joined the MEMS program at CWRU in 1994 as a Research Associate and immediately began working in the SiC MEMS area. He was promoted to Senior Research Associate in 1997 and Researcher in 2000. In addition to his research positions within the University, Dr. Zorman has held appointments as Adjunct Assistant Professor in the Department of Electrical Engineering and Computer Science and Interim Administrative Director of the Microfabrication Laboratory. He currently is an Associate Professor in EECS at CWRU. He has been instrumental in the construction of AP- and

LPCVD reactors for SiC thin films, and has led the development of recipes for the growth of single and polycrystalline 3C–SiC films for micromachined sensors and actuators. In addition to the development of novel bulk and surface micromachining techniques for SiC, Dr. Zorman was a key contributor in the development of novel polishing, wafer bonding, and low defect density growth processes for SiC. His current research interests include the development of SiC for NEMS. He has published over 120 technical papers, five book chapters, and has taught several short courses on SiC for MEMS. Prof. Zorman is a past chairman of the MEMS Technical Group in the American Vacuum Society and is currenty serving as co-chairman.